Journal of Colloid and Interface Science 526 (2018) 244–252

Contents lists available at ScienceDirect

Journal of Colloid and Interface Science

journal homepage: www.elsevier.com/locate/jcis

Regular Article

Proteolytic degradation of gelatin-tannic acid multilayers

Safiyeh Bahmanzadeh [a,b], Tautgirdas Ruzgas [a], Javier Sotres [a,*]

[a] Biomedical Science Department & Biofilms-Research Center for Biointerfaces, Malmö University, 20506 Malmö, Sweden
[b] Analytical Research Laboratory, Department of Chemistry, University of Sistan and Baluchestan, P.O. Box 98135-674, Zahedan, Iran

GRAPHICAL ABSTRACT

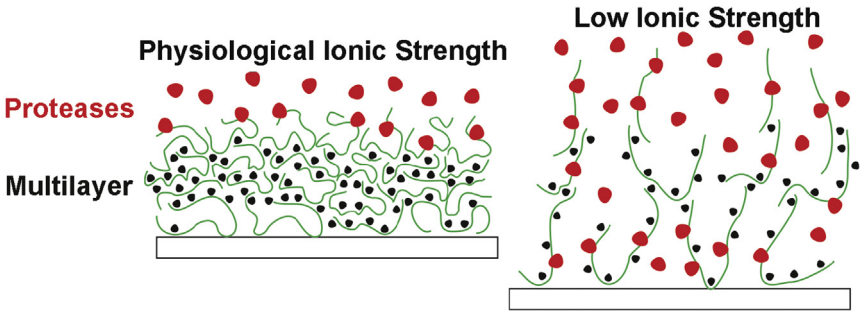

ARTICLE INFO

Article history:
Received 7 March 2018
Revised 26 April 2018
Accepted 30 April 2018
Available online 2 May 2018

Keywords:
Gelatin
Tannic acid
Biodegradable films
Edible films
Proteases
Electrochemical Impedance Spectroscopy
Quartz Crystal Microbalance with Dissipation

ABSTRACT

Hypothesis: Gelatin is one of the most popular constituents of biodegradable/edible films. Because of its poor mechanical properties, it typically needs to be cross-linked. In this regard, the use of tannic acid has attracted significant interest. Whereas the biodegradability of gelatin is well established, little is known on how different crosslinking methods affect biodegradability. In most cases, the ionic strength at which protein films are grown has a drastic effect on their structure. Thus, it is expected that by controlling the ionic strength during the growth of cross-linked gelatin films it should be possible to tune the access to relevant cleavage sites by proteases and, therefore, their biodegradability.

Experiments: Gelatin-tannic acid were grown at different ionic strengths by means of the layer-by-layer self-assembly method. The growth of these multilayers and their response to the presence of different proteases were monitored by means of Electrochemical Impedance Spectroscopy and Quartz Crystal Microbalance with Dissipation.

Findings: Gelatin-tannic acid multilayers grown at low ionic strength exhibited a swollen structure that allowed easy access to their cleavage sites by proteases. Multilayers formed at physiological ionic strength exhibited a compacter structure, which limited their proteolytic degradation.

1. Introduction

Protein films are of high interest for a wide range of applications. They stand out e.g., as ideal substitutes of the highly contaminant synthetic films. The use of synthetic packaging films is indeed the source of a major environmental problem. Due to their non-biodegradability, these materials constitute a major waste management issue with associated problems for wildlife and even for human health [1]. Thus, there is a vital need to develop biodegradable and environmentally friendly packaging materials [2]. In this regard, edible materials, specially protein films, stand out not only because of their guaranteed biodegradability, but also because of their extraordinary potential use in the food industry

* Corresponding author.
E-mail address: javier.sotres@mau.se (J. Sotres).

https://doi.org/10.1016/j.jcis.2018.04.112
0021-9797/

[3]. Beside this, protein films are of interest in many other applications such as biosensors [4,5], biofuel cells [6,7] and coatings for implants and biomedical devices [8,9]. For all these applications, it is of high relevance to understand how protein films resist proteolytic degradation as this process can reduce the performance and lifespan of the films but also ensure their biodegradability.

This work focuses on gelatin-based films. Gelatin is a protein widely used as a biomaterial in pharmaceutical, food, and medical applications [10]. Moreover, it is a renewable, biodegradable and edible material [11] that provides low gas permeability [12–14]. However, gelatin exhibits poor mechanical properties, especially when exposed to wet and/or humid conditions. To enhance its mechanical strength and water resistance, structural modifications are normally required. Specifically, this have been achieved by crosslinking gelatin with a variety of compounds e.g., formaldehyde [15]. However, many of these compounds present toxicity concerns. In order to avoid this risk, non-toxic compounds such as phenolic compounds have attracted significant interest [16]. In this regard, significant research has been performed on the use of tannic acid (TA) to crosslink gelatin [17–20] due to its ability to render films with enhanced water barrier and mechanical properties [21].

The biodegradability of gelatin is well-established [22,23]. This is obviously one of the main advantages of gelatin-based films (along with its food compatibility). Thus, it is of main importance to know whether this aspect is affected if a crosslinking method is employed to construct gelatin-based films. However, only few works have addressed the biodegradability of chemically crosslinked gelatins e.g., [24,25], and none of these studies focused on gelatin-TA films. The original aim of this work was to address this gap in knowledge. For this, we constructed gelatin-TA films at different ionic strengths by means of the layer-by-layer self-assembly method and subsequently exposed them to proteases of different origin. We monitored this process by means of Electrochemical Impedance Spectroscopy (EIS) and Quartz Crystal Microbalance with Dissipation (QCM-D). Our results evidenced that gelatin-TA films grown at physiological ionic strength exhibited a high resistance to proteolytic degradation. Thus, they are better suited for applications where a long lifespan is desirable. On the contrary, gelatin-TA films grown at low ionic strength were quickly degraded by proteases. This, along with the fact that this process could be well characterized by means of EIS, suggest that these films could be employed e.g., in bacterial/biofilms electrochemical sensors. To further explore this aspect, we also investigated the incorporation of gold nanoparticles (AuNPs) into gelatin-TA films as a way that could enhance the EIS response to the presence of proteases in solution. However, our results showed that the incorporation of AuNPS in the films drastically hindered their proteolytic degradation independently of the ionic strength at which they were grown.

2. Materials and methods

2.1. Materials

The following chemicals were purchased from Sigma-Aldrich and used without further purification: gelatin from cold water fish skin (Prod. No. G-7041), trypsin from porcine pancreas (Prod. No. T7409) and proteinase K from *Tritirachium album* (Prod. No. P5056). All other chemicals were at least of analytical grade and also purchased from Sigma-Aldrich: poly-L-Lysine hydrobromide (Prod. No. P-2636), tannic acid (Prod. No. 403040), sodium ferrocyanide decahydrate (Prod. No. 13425), potassium hexacyanoferrate (III) (Prod. No. 393517), gold (III) chloride trihydrate (Prod. No. 520918), sodium citrate dehydrate (Prod. No. W302600), phosphate buffered saline (PBS) tablets (Prod. No. P4417) and Hellmanex III (Prod. No. Z805939).

Gold nanoparticles (AuNPs) were synthesized by reduction of Gold (III) chloride trihydrate by sodium citrate dehydrate as detailed in [26]. The size and concentration of the AuNPs in water solution were ca. 28 nm (determined by Dynamic Light Scattering) and $1.44 \cdot 10^{11}$ ml^{-1} (determined from Ultraviolet–visible spectroscopy [27]) respectively.

PBS buffer was prepared from the tablets according to Sigma-Aldrich instructions resulting in 137 mM NaCl, 2.7 mM KCl and 10 mM phosphate buffer solution (pH 7.4 at 25 °C). Either solutions were prepared in this PBS buffer, or in what we named diluted PBS buffer (dPBS) were the original PBS buffer was diluted in Ultra High Quality (UHQ) water 10 times in volume.

2.2. Layer-by-layer growth of gelatin-tannic acid films

Multilayers were grown from gelatin, tannic acid (TA) and poly-l-lysine (PLL) solutions at a 0.1 mg ml^{-1} concentration in either PBS or dPBS buffer (each experiment was performed by using a single type of buffer). Immediately after preparation, all solutions were stored at -20 °C and only thawed just before being used. For building the multilayers, a PLL solution was initially flowed through the experimental chamber during 10 min, then flow was stopped and the layer stabilized for another 10 min and finally the specific buffer of the experiment was rinsed for an additional 10 min period. Then, gelatin and tannic acid multilayers were formed by following the same time steps i.e., 10 min flow of the solution, 10 min stabilization under non-flow conditions and 10 min rinsing with the specific buffer used in the experiment. Multilayers were grown until a 5th gelatin layer was adsorbed. In some experiments this was followed by 20 min exposure of the multilayer to a protease solution (trypsin or proteinase K) at a concentration of 0.1 mg ml^{-1}; always in PBS buffer (independently of the buffer used for building the multilayers). In some other experiments, exposure to the proteases was preceded by the adsorption of gold nanoparticles (AuNPs). This was done by flowing over the 5th gelatin layer the AuNPs in UHQ water solution specified above for 10 min followed also by a 10 min stabilization period and a 10 min rinsing in the specific buffer of the experiment.

2.3. Electrochemical Impedance Spectroscopy (EIS)

Electrochemical impedance spectroscopy (EIS) measurements were conducted with an Inter-Digitated gold Electrodes (IDEs) (G-IDEAU10, DropSens, Llanera, Spain) placed in a flow chamber. G-IDEAU10 comprised 250 × 2, 10 μm broad, electrode fingers with 10 μm gap in between. The IDE was connected in two-electrode configuration to a potentiostat (Iviumstat, Ivium Technologies, Eindhoven, The Netherlands). EIS was run in a frequency range from 1 Hz to 0.1 MHz with five frequencies per decade. The amplitude of the applied alternating voltage was 0.02 V, DC voltage was 0 V.

For EIS experiments, multilayers were grown as specified above, with the difference that the buffer used in each rinsing step contained 1 mM $Na_4[Fe(CN)_6]$ and 1 mM $K_3[Fe(CN)_6]$ to enable the EIS measurement after each rinsing step. Results were fitted to an equivalent circuit model consisting on a solution resistance (R_S) connected in series with a parallel combination of a constant phase element (CPE) and charge transfer resistance (R_{CT}). CPE accounts for the electric double layer capacitance at the electrodes–electrolyte interface, and a charge transfer resistance reflected the heterogeneous charge transfer process between the redox reagent in solution and the surface of the IDE electrode [28]. Fittings were performed by means of the IviumSoft software (Ivium Technologies, Eindhoven, The Netherlands).

2.4. Quartz Crystal Microbalance with Dissipation (QCM-D)

Quartz Crystal Microbalance with Dissipation (QCM-D) measurements were performed by using an E4 system (Q-Sense AB, Sweden). A detailed description of the technique and its basic principles can be found elsewhere [29]. Briefly, an alternating-current voltage is applied through a gold-coated quartz chip to stimulate the shear mode oscillation of the quartz crystal. Specifically, in our experiments we used gold-coated AT-cut piezoelectric quartz crystals (QSX 301, Q-Sense AB, Sweden). Adsorption of a certain amount of mass, Γ, onto the sensor surface leads to a decrease in the frequency of the resonance overtones, f_n. Along with the shifts in f_n, QCM-D is able to detect changes in the dissipation factor, D_n, of each of the overtones [30]. The dissipation factor represents the ratio between the energy dissipated by the sensor during a single oscillation after switching off the driving voltage, and the initial oscillation energy of the sensor.

If the adsorbed layer is rigid enough so that the dissipation factor D_n can be neglected, the shifts in f_n scaled by the overtone number n are linearly related by means of the Sauerbrey equation [31]:

$$\frac{\Delta f_n}{n} = -\frac{2\Gamma f_0^2}{z_q} \tag{1}$$

where n is the overtone number, Δf_n the frequency shift of the nth overtone, Γ is the adsorbed amount, f_0 is the quartz fundamental frequency and Z_q its acoustic or mechanical impedance. It can be noted that within the Sauerbrey approximation, a similar mass would be obtained from the analysis of all overtones. However, the multilayers may exhibit a viscoelastic character instead. For viscoelastic films, $\Delta f_n/n$ exhibit a dependence with n and the dissipation factor, ΔD_n, are not negligible. In this case, the Sauerbrey approximation usually underestimates the areal mass, and the Voigt model provides more accurate values. The expressions obtained by applying the Voigt model for a viscoelastic film at a solid/liquid interface are [32]:

$$\Delta f_n/f_n = -\frac{d_p\rho_p}{d_Q\rho_Q}\left[1-\eta_l\rho_l\frac{\left(\eta_p/\rho_p\right)\omega_n}{\mu_p^2+\omega_n^2\eta_p^2}\right] = -\frac{\Gamma_p}{d_Q\rho_Q}\left[1-\eta_l\rho_l\frac{\left(\eta_p/\rho_p\right)\omega_n}{\mu_p^2+\omega_n^2\eta_p^2}\right] \tag{2a}$$

$$\Delta D_n = \frac{1}{d_Q\rho_Q}\left[\eta_l\rho_l\frac{d_p\mu_p\omega_n^2}{\mu_p^2+\omega_n^2\eta_p^2}\right] \tag{2b}$$

In these equations d, ρ, and ω_n stand for thickness, density, and $2\pi f_n$ respectively. The subscripts Q, p, and l stand for quartz crystal, protein film, and liquid medium respectively. In this work, the D-Find software (Q-Sense AB, Sweden) was used to fit experimental data with both the Sauerbrey and Voigt models. For both fits, the overtones 5, 7 and 9 were used. For the case of Sauerbrey mass, this meant that for every time point of the experiment, the provided adsorbed amount is the average resulting from applying Eq. (1) to each of these overtones.

Before every experiment, sensors were rinsed extensively with UHQ water, treated in a Hellmanex II 2% (v/v) water solution for 10 min. and subsequently rinsed again extensively with UHQ water. Finally, before being used, the sensors were dried under nitrogen and plasma-cleaned for 5 min in low-pressure residual air using a glow discharge unit (PDC-32 G, Harrick Scientific Corp., USA). Clean sensors were then placed in QCM-D chambers thermostated to 25 °C. Liquid solutions were supplied into the QCM-D chamber using an Ismatec peristaltic pump IPC-N 4 at a flow rate of 0.1 ml min^{-1}. In the beginning, the chambers were filled with the buffer that would be used for building the multilayers (PBS or dPBS). After stable frequency and dissipation signals were observed, gelatin-TA multilayers were growth by flowing appropriate solutions following the protocol detailed above.

3. Results

3.1. Electrochemical Impedance Spectroscopy (EIS)

The growth of gelatin-TA multilayers at different ionic strengths and their resistance to proteolytic degradation was investigated by means of EIS. Fig. 1a shows a Nyquist plot for a representative experiment were a gelatin-TA multilayer was grown on a PLL-coated Au electrode in diluted PBS buffer. Adsorption of an initial PLL was required in order to increase sensitivity of EIS, probably by preventing denaturation of gelatin on the Au surface. Fig. 1 also

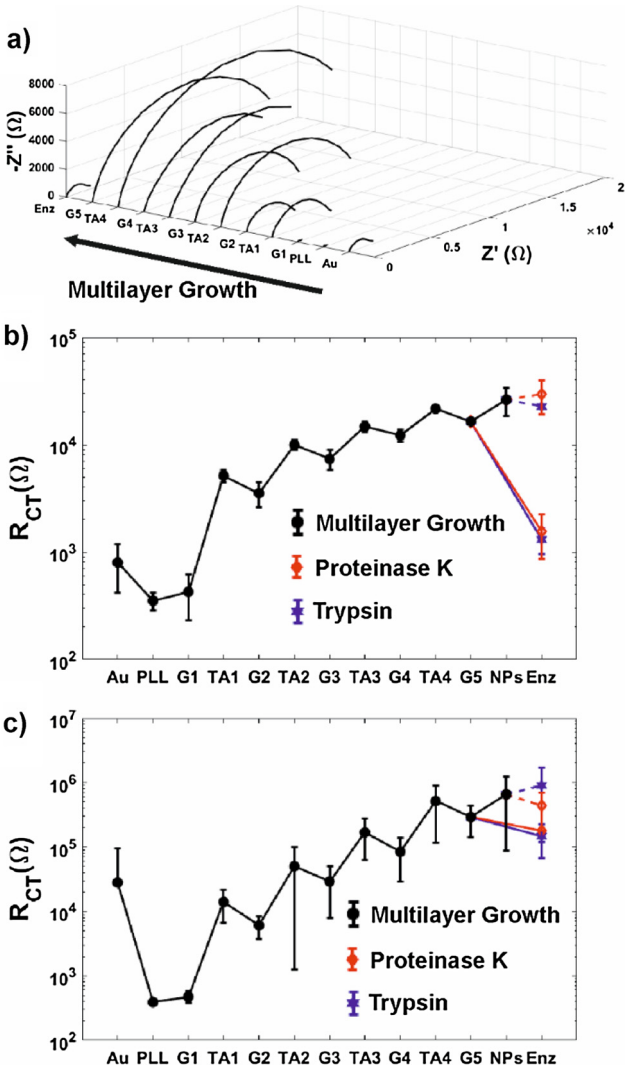

Fig. 1. (a) Nyquist plots for a representative growth of a gelatin-TA multilayer on PLL-coated gold treated with protease K in the end of the experiment. (b) and (c) Average R_{CT} values for the growth of the multilayers in dPBS and PBS buffers respectively. Data corresponding to the multilayers growth were calculated from 4 different experiments, whereas data for the multilayers rinsed with each of the enzymes were calculated from 2 different experiments. *G1-5* note the system after the deposition of the 1st to the 5th layers of gelatin. *T1-4* note the 1st to the 4th layers of TA intercalated between the gelatin layers. *NPs* notes the adsorption of gold nanoparticles. *Enz* notes the multilayers after being treated with a given protease. This nomenclature is maintained in all other figures of the manuscript.

shows the drastic effect of exposing the multilayer to a protease (proteinase K in this specific case) solution.

For every layer, EIS data was fitted to an equivalent circuit model consisting of a solution resistance connected in series with the parallel combination of a constant phase element and a charge transfer resistance (see Section 2). The charge transfer resistance, R_{CT}, results from the charge transfer process between the redox reagents and the electrodes. Thus, we have used this parameter to characterize the growth of the multilayers and their behavior upon the exposure to proteases. Fig. 1b shows average R_{CT} values obtained for the multilayers grown in diluted PBS (dPBS) buffer. Fig. 1c shows similar results but for multilayers grown in PBS buffer (i.e., physiological ionic strength). Overall, data shows that at both investigated ionic strengths R_{CT} increases along with the number of gelatin-TA deposition cycles. However, when grown at physiological ionic strength the multilayers showed significantly (approx. 10 times) higher resistance to heterogeneous redox conversion of ferri/ferrocyanide at the electrode surface.

The ionic strength at which the multilayers were grown had as well an effect on their resistance to proteolytic degradation. When grown at low ionic strength, R_{CT} could be significantly decreased upon the exposure of the multilayers to the proteases trypsin and proteinase K (Fig. 1b). However, the decrease was significantly lower when the multilayers were grown at physiological ionic strength (Fig. 1c). Specifically, for the multilayers grown at low ionic strength, the ratio between R_{CT} calculated after and before the exposure to the proteases was 0.08 ± 0.02 in the case of trypsin and 0.09 ± 0.04 in the case of proteinase K. For the multilayers grown at physiological ionic strength, the corresponding ratio between R_{CT} values after and before the exposure to the proteases was 0.56 ± 0.01 in the case of trypsin and 0.57 ± 0.37 in the case of proteinase K.

We also monitored by means of EIS the adsorption of AuNPs on the multilayers and how this affected proteolytic degradation (data included in Fig. 1b and c). Specifically, EIS revealed that the adsorption of AuNPs on top of the multilayers had a relatively small effect on R_{CT} i.e., for both type of multilayers it led to a change similar to that observed after adding TA in the previous growth steps. However, this had a drastic effect on the resistance to proteolytic degradation of the multilayers. Fig. 1b and c also show that the multilayers covered with AuNPs were almost unaffected when exposed to proteases, independently of the ionic strength at which they were grown.

3.2. Quartz Crystal Microbalance with Dissipation (QCM-D)

In order to gain further mechanistic insight into the structure of gelatin-TA multilayers and on how it affects their resistance to

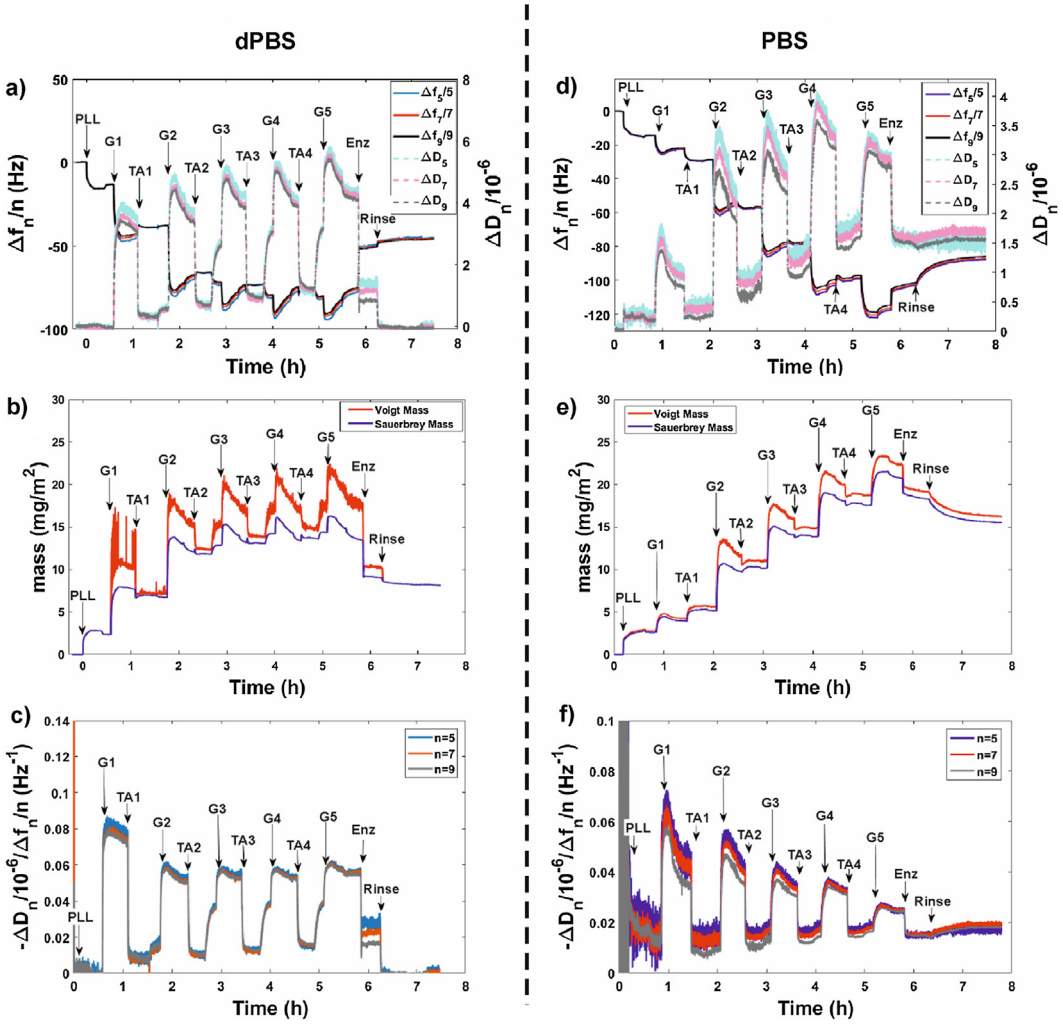

Fig. 2. (a) Frequency and dissipation shifts for the 5th, 7th and 9th overtones corresponding to a representative experiment where gelatin-TA multilayers were grown in diluted PBS buffer followed by rinsing with a proteinase K solution. (b) Sauerbrey and Voigt masses and (c) $-\Delta D_7/\Delta f_7$ calculated from the data in (a). (d) Frequency and dissipation shifts for the 5th, 7th and 9th overtones corresponding to a representative experiment where gelatin-TA multilayers were grown in PBS buffer with physiological ionic strength followed by rinsing with a proteinase K solution. (e) Sauerbrey and Voigt masses and (f) $-\Delta D_7/\Delta f_7$ calculated from the data in (d).

protease degradation, these systems were investigated by means of QCM-D. Specifically, we report here studies on multilayers built on top of a PLL-coated gold surface i.e., on the same type of multilayers investigated by means of EIS so that results from both techniques could be compared. Nevertheless, we also investigated by means of QCM-D gelatin-TA multilayers built directly on gold surfaces (Supplementary Information, Fig. S1), and no major differences with respect to those built on top of a PLL layer were found.

QCM-D results from representative experiments are shown in Fig. 2. Fig. 2a shows frequency and dissipation shifts for the 5th, 7th and 9th overtones corresponding to a representative experiment where gelatin-TA multilayers were grown in diluted PBS buffer and then rinsed with a proteinase K solution. It can be observed that most of frequency and dissipation shifts occur during the formation of the PLL layer and during the two initial gelatin-TA deposition cycles. Adsorption of additional layers led to significantly lower frequency shifts indicating the difficulty for the multilayers to grow any further. Dissipation shifts followed a slightly similar trend, even though for this signal it is clear how higher values were observed after the addition of gelatin than after the addition of TA for any of the deposition cycles.

We used both the Sauerbrey (Eq. (1), the plotted mass at any time point is the average from the Sauerbrey masses obtained for the 5th, 7th and 9th overtones) and Voigt (Eqs. (2a) and (2b)) models to estimate the areal mass of the multilayers. Fig. 2b shows the results for this modelling for multilayers grown in diluted PBS buffer. In this situation, because of the low ΔD values, the Voigt model could not be used to fit the initial PLL layer and the rinsed multilayers after their exposure to proteases. This was possible instead for the rest of the experimental intervals, and a comparison between the results from both models indicated (as expected) that the Sauerbrey mass underestimated the Voight mass. Nevertheless, results from both models exhibited a similar trend. In consequence, results from the Sauerbrey model were used to discuss the areal mass of the multilayers. Fig. 3a shows the average Sauerbrey mass corresponding to each of the steps of the growth of the multilayers in diluted PBS buffer calculated from eight different experiments. This figure shows that addition of the first gelatin layer gave rise to a significant increase in the adsorbed mass, which was lowered when adsorbing TA on top. A similar behavior was observed for the second deposition cycle. However, further deposition cycles only led to very low changes in the adsorbed mass, even though an increasing trend was still observed.

Dissipation shifts are associated not only with the viscoelasticity of the adsorbed material but also with changes in mass [33]. Still, a simple way to qualitatively describe the viscoelasticity of the adsorbed material is to analyze the ratio between frequency and dissipation shifts, $-\Delta D/\Delta f$ [34,35]. Higher values for this ratio indicate a higher viscous character. Fig. 2c shows the evolution of $-\Delta D/\Delta f$ during the formation of the multilayers for the 5th, 7th and 9th overtones. Fig. 3b shows, for the 7th overtone, the average of this ratio after each rinsing step calculated from eight different experiments. This data revealed that the adsorption of gelatin led to a significant increase of the viscous character of the multilayers whereas this character significantly decreased after TA adsorption. Nevertheless, when considering gelatin-TA deposition cycles as a whole, $-\Delta D/\Delta f$ exhibited a trend indicating that a higher number of deposition cycles leads to more viscous multilayers (Figs. 2c and 3b).

The exposure of the multilayers grown at low ionic strength to the proteases trypsin and proteinase K significantly reduced both their mass and viscous character (Fig. 3a and b). Specifically the ratio between the Sauerbrey masses after and before the exposure to the proteases was 0.48 ± 0.15 for trypsin and 0.59 ± 0.18 for proteinase K, whereas the ratio between the corresponding $-\Delta D_7/\Delta f_7$ was 0.25 ± 0.07 for trypsin and 0.28 ± 0.10 for proteinase K.

The multilayers exhibited a different structure when grown at physiological ionic strength (PBS buffer). In this case, the frequency shifts (Fig. 2d) and the corresponding adsorbed masses (Figs. 2e

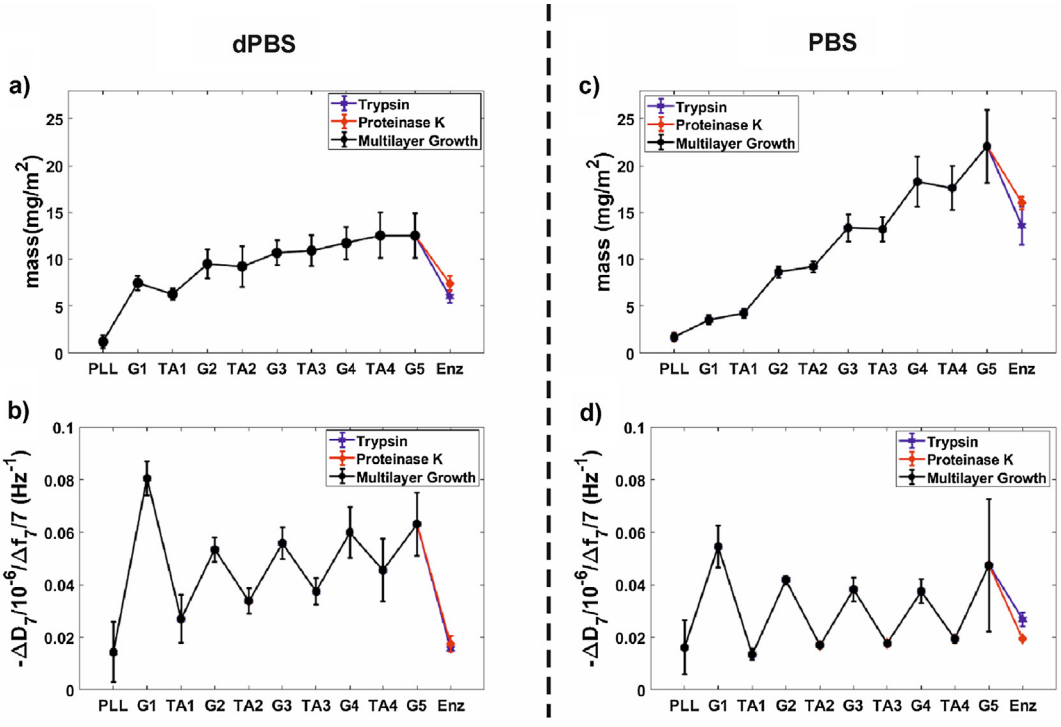

Fig. 3. (a) Sauerbrey mass and (b) $-\Delta D_7/\Delta f_7$ values for the building of gelatin-TA multilayers on PLL coated gold surfaces in diluted PBS buffer (low ionic strength) and rinsed with both trypsin and proteinase K solutions. (c) Sauerbrey mass and (d) $-\Delta D_7/\Delta f_7$ values for the building of gelatin-TA multilayers on PLL coated gold surfaces in PBS buffer (physiological ionic strength) and rinsed with both trypsin and proteinase K solutions. Data corresponding to the multilayers growth were calculated from 8 different experiments, whereas data for the multilayers rinsed with each of the enzymes were calculated from 2 different experiments.

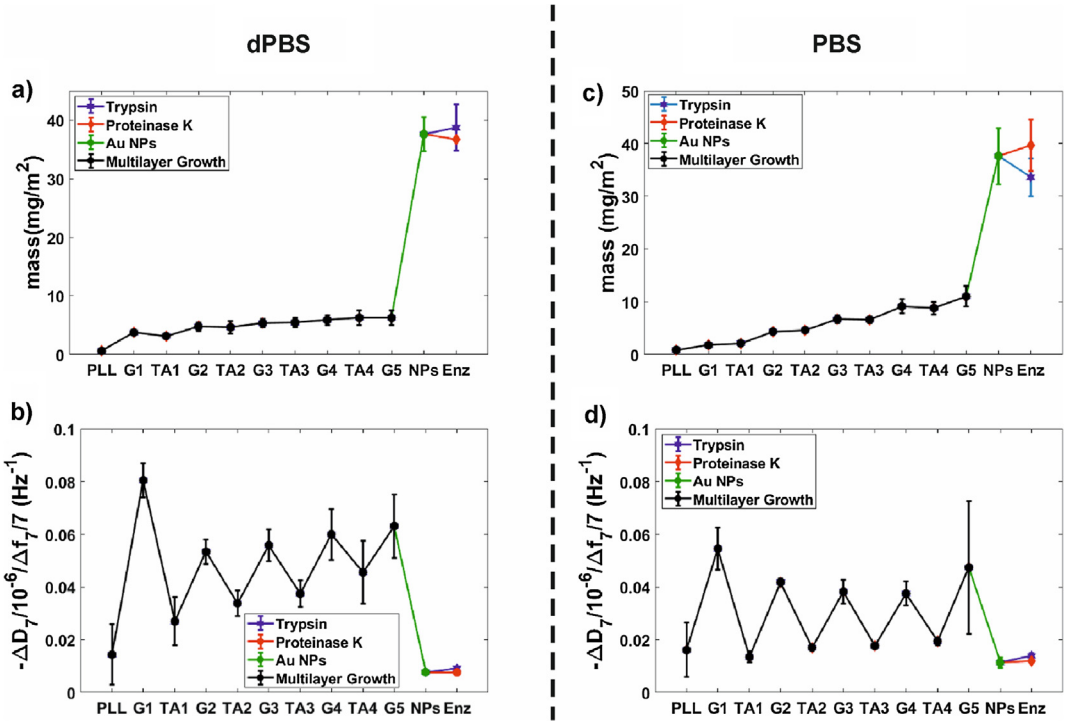

Fig. 4. (a) Sauerbrey mass and (b) $-\Delta D_7/\Delta f_7$ values for the building of gelatin-TA multilayers, in diluted PBS buffer (low ionic strength), covered with an AuNPs layer and finally rinsed with both trypsin and proteinase K solutions. (c) Sauerbrey mass and (d) $-\Delta D_7/\Delta f_7$ values for the building of gelatin-TA multilayers in PBS buffer (physiological ionic strength), covered with an AuNPs layer and finally rinsed with both trypsin and proteinase K solutions. Data corresponding to the multilayers growth were calculated from 8 different experiments, whereas data for the multilayers rinsed with each of the enzymes were calculated from 2 different experiments.

and 3c) indicated that the growth of the multilayers exhibited a linear behavior, even though addition of TA from the third deposition cycle led to a subtle decrease in mass in relation to that of the previous gelatin layer. This behavior can be clearly observed in Fig. 3e which shows the average of the Sauerbrey mass after each rinsing step calculated from eight different experiments. Regarding the viscoelastic indicator $-\Delta D/\Delta f$, Fig. 2f shows that gelatin adsorption increased the viscosity of the multilayers while addition of TA reduced it. Whereas it could be inferred from Fig. 2f that the effect of gelatin adsorption on the $-\Delta D/\Delta f$ signal decreased as the number of deposition cycles increased, this was not a reproducible behavior. As seen in Fig. 3d, which shows the average $-\Delta D_7/\Delta f_7$ value after each rinsing step calculated from eight different experiments, after the second gelatin/tannic acid double layer the effect of either gelatin or tannic acid adsorption on the overall $\Delta D/\Delta f$ ratio did not exhibit a clear dependence with the number of previously adsorbed layers.

The ionic strength at which the multilayers were grown also had a significant effect on their ability to resist protease degradation. While the exposure to proteases of the multilayers grown at physiological ionic strength led to a decrease of their mass and viscous character, this decrease was smaller than that observed for the multilayers grown at low ionic strength. Specifically, for the multilayers grown at physiological strength, the ratio between the Sauerbrey masses calculated after and before the exposure to the proteases was 0.62 ± 0.20 in the case of trypsin and 0.73 ± 0.16 in the case of proteinase K. The corresponding ratio between the $-\Delta D_7/\Delta f_7$ values after and before the exposure to the proteases was 0.57 ± 0.36 in the case of trypsin and 0.41 ± 0.24 in the case of proteinase K. At this point, it is worth to note that whereas for the multilayers grown at low ionic strength exposure to the proteases for 20 min led to stable frequency and dissipation shifts, this was not the case for the multilayers built at physiological ionic strength. Even though in this case the rate at which mass decreased was already significantly small after the investigated 20 min period, it was not zero. Thus, our data does not imply that the multilayers built at physiological strength are not biodegradable. It indicates instead that the biodegradation process would take over a significantly longer period than for the multilayers grown at low ionic strength.

The interaction of AuNPs with gelatin-TA multilayers, and their effect on their degradation by proteases was also investigated by means of QCM-D. The average values for the Sauerbrey mass and $-\Delta D_7/\Delta f_7$ ratio calculated from four different experiments for both diluted PBS and PBS buffer are shown in Fig. 4. When gelatin-TA multilayers grown both in PBS and in diluted PBS buffer were exposed to a $1.44 \cdot 10^{11}$ ml^{-1} in water solution of AuNPs for 20 min, and subsequently rinsed with the same buffer used while building them, the areal masses of both systems reached a similar value of ca. 8 mg m^{-2}. Adsorption of AuNPs also led to highly elastic (low viscous) multilayers as indicated by the significant decrease in $-\Delta D/\Delta f$, Moreover, as shown as well in Fig. 4, exposure to the proteases trypsin and proteinase K had a negligible effect on the multilayers covered by AuNPs.

4. Discussion

The interaction between gelatin and TA has been extensively described in the literature. Under alkaline conditions, ionic and covalent forces may mediate the interaction between both compounds [19]. However, at physiological and acidic pH conditions it is more likely that this interaction is mediated by hydrophobic and hydrogen bond forces [18,20]. Specifically, the hydrophobic amino acid side chains on gelatin could develop hydrophobic interactions with the aromatic rings of galloyl units on TA. Subsequently, hydrogen bonds could be formed between phenolic hydroxyl groups on TA and carbonyl groups on gelatin molecular chains. The same forces that mediate the interaction between both compounds will also drive the layer-by-layer growth of gelatin-TA

multilayers. However, the fact that at neutral and acidic pH conditions gelatin and TA do not interact through electrostatic forces does not imply that ionic strength does not play a role in the structure of gelatin-TA multilayers grown in these conditions. Ringwald and co-workers [18] investigated the role of ionic strength in the formation of gelatin-TA multilayers at pH 5. TA has a pKa close to 8.5 [36]. Therefore, its interaction at pH 5 with gelatin should not be influenced by the ionic strength. However, they observed that higher multilayer thicknesses were obtained at lower ionic strength. This was attributed to the effect of ionic strength on the conformation of gelatin. The isoelectric point of the gelatin that they used was reported to be ca. 4.9 i.e., it would be slightly charged. Therefore, at low ionic strength gelatin would exhibit a more swollen conformation due to the electrostatic repulsion between its charged moieties. This would in turn lead to the observed higher thickness of the gelatin-TA multilayers.

In contrast with the results from Ringwald and co-workers [18], our experiments showed that higher thickness of the gelatin-TA multilayers were obtained at higher ionic strength. This was so even though our experiments were also performed at conditions i.e., pH 7.4, where TA would not be electrostatically charged and would, therefore, not develop electrostatic interactions with gelatin. Indeed, under low ionic strength conditions (diluted PBS buffer) we observed that the mass of the multilayers hardly changed after the second gelatin-TA deposition cycle. In contrast, the mass of the multilayers grown at physiological ionic strength (PBS buffer) exhibited a linear dependence with the number of deposition cycles. However, our results do not really contradict those reported by Ringwald and co-workers [18] as discussed below.

Focusing on our results at low ionic strength, gelatin readily adsorbed on the initial PLL layer. Our experiments were performed at pH 7.4. The isoelectric point of the gelatin employed in this work was approximately 6 (information provided by the manufacturer). Thus, gelatin develops a net (negative) charge in these conditions. Therefore, its high affinity for PLL, a cationic polypeptide, can be explained by means of electrostatic interactions. When the first gelatin layer was exposed to TA, the overall QCM-D mass decreased. However, QCM-D mass includes that of the adsorbed material and that of the coupled solvent [37,38], so that it is often referred as "wet mass". Thus, a decrease in QCM-D mass does not necessarily imply desorption of material from the sensor surface. It can also be the result from dehydration, which was more likely the case in our experiments. This is supported by the fact that exposure to TA led to a significant decrease of the viscous character of the multilayers i.e., lower $-\Delta D/\Delta f$ values (Fig. 3b). The same is supported by the observed higher resistance to the access of ferricyanide and ferrocyanide ions to the electrode surface i.e., higher R_{CT} values (Fig. 1b). Thus, our results indicate that TA bound to the first gelatin layer and that this resulted in a compacter structure and in a release of trapped solvent up to an amount that surpassed the mass of adsorbed TA molecules. A subsequent layer of gelatin could still be adsorbed, which could be again compacted by the addition of TA. However, further deposition cycles only resulted in a subtle increase of the multilayer mass. This can be explained by the strong and long-ranged inter and intra-molecular electrostatic repulsion expected between the charged gelatin molecules at low ionic strength. The fact that the second deposition cycle resulted in a significant increase of the adsorbed mass can be explained by the presence of the inner cationic PLL layer. This layer could counteract the electrostatic repulsive forces by which the already adsorbed gelatins would repeal the incorporation of further gelatins into the multilayer. This was supported by the fact that if an initial PLL was not used to construct the multilayers, their growth was already hindered after the first deposition cycle, (Supporting Information, Fig. S1). However, the multilayer thickness after the second deposition cycle (ca. 10 nm if we assume a density of 1 g/ml) is already significantly higher than the Debye length of the diluted PBS buffer (<3 nm). Thus, gelatin molecules facing the surface after the second deposition cycle would not be attracted by the underlying PLL layer. In this scenario, their repulsive interaction with the already adsorbed gelatin would limit their incorporation to the multilayer as experimentally observed (Fig. 3a). Most likely, Ringwald and co-workers [18,20] managed to build gelatin-TA multilayers at low ionic strength because they operated at a pH only slightly higher than the isoelectric point of the used gelatin. In this way, they minimized the long-range electrostatic repulsion that, in our case, prevented the multilayer growth.

At physiological strength, a different scenario was found. The first deposition cycle resulted in a lower QCM-D mass than that observed at low ionic strength. This was the result of the highly swollen conformation of the gelatin molecules at low ionic strength, which entailed a high amount of entrapped solvent. At physiological ionic strength, gelatin molecules would be more coiled as a result of the screening of the electrostatic repulsion between them. This entailed a lower amount of entrapped solvent and, therefore, of QCM-D mass. However, from the second deposition cycle the mass of the multilayers built at physiological strength surpassed that of those built at low ionic strength. This indicates that the screening of electrostatic interactions at these conditions allowed the incorporation of gelatin to the multilayers for all monitored deposition cycles. Indeed, at physiological ionic strength the adsorbed mass increased in an approximately linear way with the number of deposition cycles (Fig. 3c). A linear growth indicates that the adsorbing species deposit on the outer surface with little interlayer diffusion [39]. This suggests that after each deposition cycle, a well-defined gelatin-TA layer was formed, which was supported by the fact that the $-\Delta D/\Delta f$ values after the addition of either gelatin or TA did not exhibit a clear dependence with the deposition cycle (Fig. 3d). Focusing on each deposition cycle, we observed that, in the same way observed for the multilayers built at low ionic strength, the incorporation of gelatin lead to swollen layers subsequently compacted by the addition of TA (which supports its crosslinking ability).

We investigated the resistance to proteolytic degradation of gelatin-TA multilayers, built both at low and physiological ionic strength, by exposing them for 20 min to trypsin and proteinase K solutions in PBS buffer. We observed that the layers built at low ionic strength were significantly degraded. This was inferred by the decreased in the adsorbed mass from QCM-D experiments: 52% for trypsin and 41% for proteinase K (Fig. 3a). The effective R_{CT} of the multilayers obtained by EIS also decrease by ca. one order of magnitude after the exposure to the proteases (Fig. 1b). The multilayers built at physiological ionic strength were significantly more resistant to proteolytic degradation. After their exposure to the proteases, their mass as determined by means of QCM-D was lowered by 38% in the case of trypsin and 27% in the case of proteinase K, and their effective R_{CT} hardly changed (Fig. 1c). These results can be explained by the structural properties of the multilayers discussed above. In the multilayers built at physiological ionic strength (PBS buffer), gelatin molecules would be highly coiled not only because of their reduced intra-molecular repulsion but also probably because they wrapped around TA molecules [20]. This led to a very compact structure that not only prevented inter-diffusion of the material adsorbed during each deposition cycle, but also limited protease access to susceptible cleavage sites. The multilayers built at low ionic strength (diluted PBS buffer) exhibited a highly swollen structure instead. This was supported by the fact that after each deposition cycle, their R_{CT} values were significantly lower, and their $-\Delta D/\Delta f$ values significantly higher, than those exhibited by multilayers built at physiological ionic strength. Thus, the investigated proteases could easily access their

corresponding gelatin cleavage sites when exposed to the swollen multilayers built at low ionic strength and, therefore, degrade them almost immediately.

Our results indicate that gelatin-TA films built a higher ionic strength exhibited a significantly higher resistance to proteolysis. However, this does not imply that they are not biodegradable, as stable mass values were not achieved within our experimental times. Our results indicate instead that proteolytic degradation of these multilayers takes place over periods much longer than for multilayers built at low ionic strength, which were degraded almost immediately after the exposure to proteases. Thus, gelatin-TA films grown at high ionic strengths are better suited for applications such as edible packaging where an ability to resist biological degradation for a long time is desirable.

The fact that EIS could monitor how gelatin-TA multilayers built at low ionic strength were almost immediately degraded upon exposure to proteases is also of high interest. As reported, exposure to 20 min to a protease solution led to a decrease of one order of magnitude of the effective R_{CT} of the multilayers. This opens the possibility of using this degradation as a sensing mechanism for electrochemically based sensors for e.g., bacteria and biofilms.

With this in mind, we tested a new approach to increase the sensitivity of gelatin-TA multilayers as biosensors. We coated the multilayers with AuNPs. By means of this approach, we expected that the proteases would still be able to degrade the gelatin-TA layers so that the NPs would collapse leading to an even higher decrease of the effective R_{CT} of the systems. However, this was not the case. As shown, AuNPs exhibited a high affinity for gelatin-TA multilayers independently of the ionic strength at which they were grown. After being exposed to AuNPs, the monitored QCM-D mass rapidly reached a stable value higher than that of the multilayers by ca. 60–65 mg m^{-2} (Fig. 4), indicating an effective surface coverage. Their corresponding $-\Delta D/\Delta f$ values went down as well to values lower than that of the initial PLL layer indicating an extremely low viscous character. This could be attributed to the fact that the AuNPs dominated the viscoelastic behavior of the multilayers, and not to a structural change of the underlying gelatin-TA multilayers. This was supported by the fact that the adsorption of AuNPs did not drastically alter the access of the fericyanide and ferrocyanide ions to the surface i.e., their effective R_{CT}. When exposed to the proteases, the films coated with AuNPs were almost unaltered (Fig. 1b and c and Fig. 4). This implies that AuNPs almost completely prevented the diffusion of proteases within the underling gelatin-TA films. Further studies are needed in order to unravel the underlying mechanisms by which AuNPs prevented the proteolytic degradation of gelatin-TA multilayers. However, it is reasonable to expect that this was partly due to the AuNPs forming a steric barrier to the proteases, which could probably adsorb on the AuNPs surfaces as well.

Thus, coating gelatin-TA films with AuNPs drastically increased their resistance to proteolytic degradation. This setup might be of not very much use for sensing purposes. However, the use of nanoparticles in food packaging as a way to reinforce their barrier and mechanical properties has lately attracted significant interest [40]. Because of their cost, AuNPs might not be ideal candidates. However, it is reasonable to expect that other types of particles e.g., silica nanoparticles, would prevent proteolytic degradation in a similar way and could be used to extend the shelf life of edible films.

5. Conclusions

A first conclusion of this work is that it is possible to grow, by means of the layer-by-layer self-assembly method, gelatin-TA multilayers at physiological pH at both low and physiological ionic strength. However, at low ionic strength the growth of the multilayers proceeds at a significant slower rate with respect to the number of deposition cycles. This is a consequence of the intermolecular repulsion between gelatin molecules. At physiological ionic strength, where this electrostatic repulsion is screened, the multilayers exhibit instead a linear growth with the number of deposition cycles.

This work was motivated by the hypothesis that the biodegradability of edible films could be tuned by controlling the ionic strength at which they are built. Our findings confirmed this hypothesis i.e., the ionic strength conditions during the growth of gelatin-TA multilayers had a critical effect on their resistance to proteolytic degradation. Gelatin-TA multilayers built at low ionic strength were almost completely degraded upon exposure to proteases whereas those built at physiological strength exhibited a significant resistance to proteolytic degradation. This could be attributed to the electrostatic repulsion between gelatin molecules. The long-ranged electrostatic repulsion present between the gelatin molecules while growing the multilayers at low ionic strength resulted in a swollen structure that allowed proteases to access gelatin cleavage sites. However, at physiological strength, the screening of these electrostatic interactions led to multilayers with a compact structure that limited protease access.

These findings indicate that the ionic strength during the construction of protein films could be a key parameter to optimize their performance for different applications. On the one hand, gelatin-TA films built at high ionic strengths are better suited for applications such as edible packaging where an ability to resist biological degradation for long periods is desirable. We also showed that coating gelatin-TA multilayers with Au nanoparticles completely prevented proteolytic degradation. This suggests that coating biodegradable films with nanoparticles could lead to films of extended shelf life, a research line that is worth further investigations. On the other hand, the fact that gelatin-TA multilayers grown at low ionic strength were almost immediately degraded upon the exposure to proteases, and that this degradation could be monitored by means of EIS, opens the possibility to use these multilayers in electrochemically based sensors for e.g., bacterial/biofilms. This is, the presence of bacteria/biofilms in the ambient medium could be detected by means of impedance changes resulting from the degradation of gelatin-TA multilayers grown on electrode surfaces.

Acknowledgements

Financial support from the Knowledge Foundation (grant number 20150207), the Biofilms-Research Center for Biointerfaces and Malmö University is gratefully acknowledged.

Appendix A. Supplementary material

Supplementary data associated with this article can be found, in the online version, at https://doi.org/10.1016/j.jcis.2018.04.112.

References

[1] R.C. Thompson, S.H. Swan, C.J. Moore, F.S. Vom Saal, Our plastic age, Philos. Trans. R. Soc. B 364 (2009) 1973–1976.
[2] J.H. Song, R.J. Murphy, R. Narayan, G.B.H. Davies, Biodegradable and compostable alternatives to conventional plastics, Philos. Trans. R. Soc. Lond. B 364 (2009) 2127–2139.
[3] A.E. Pavlath, W. Orts, Edible films and coatings: why, what, and how? in: K.C. Huber, M.E. Embuscado, (eds.), Edible Films And Coatings For Food Applications, Springer, New York, New York, Ny, 2009, pp 1–23.
[4] E.E. Ferapontova, V.G. Grigorenko, A.M. Egorov, T. Börchers, T. Ruzgas, L. Gorton, Mediatorless biosensor For H2o2 based on recombinant forms of horseradish peroxidase directly adsorbed on polycrystalline gold, Biosens. Bioelectron. 16 (2001) 147–157.

[5] T. Hianik, M. Šnejdárková, L. Sokolíková, E. Meszár, R. Krivánek, V. Tvarožek, I. Novotný, J. Wang, Immunosensors based on supported lipid membranes, protein films and liposomes modified by antibodies, Sens. Actuator B-Chem. 57 (1999) 201–212.
[6] M. Falk, V. Andoralov, Z. Blum, J. Sotres, D.B. Suyatin, T. Ruzgas, T. Arnebrant, S. Shleev, Biofuel cell as a power source for electronic contact lenses, Biosens. Bioelectron. 37 (2012) 38–45.
[7] D. Pankratov, R. Sundberg, J. Sotres, I. Maximov, M. Graczyk, D.B. Suyatin, E. González-Arribas, A. Lipkin, L. Montelius, S. Shleev, Transparent and flexible, nanostructured and mediatorless glucose/oxygen enzymatic fuel cells, J. Power Sources 294 (2015) 501–506.
[8] A. Sachse, A. Wagner, M. Keller, O. Wagner, W.D. Wetzel, F. Layher, R.A. Venbrocks, P. Hortschansky, M. Pietraszczyk, B. Wiederanders, H.J. Hempel, J. Bossert, J. Horn, K. Schmuck, J. Mollenhauer, Osteointegration of hydroxyapatite-titanium implants coated with nonglycosylated recombinant human bone morphogenetic protein-2 (Bmp-2) in aged sheep, Bone 37, pp. 699–710.
[9] M. Torculas, J. Medina, W. Xue, X. Hu, Protein-based bioelectronics, ACS Biomater. Sci. Eng. 2 (2016) 1211–1223.
[10] K.B. Djagny, Z. Wang, S. Xu, Gelatin: a valuable protein for food and pharmaceutical industries: review, Crit. Rev. Food Sci. Nutr. 41 (2001) 481–492.
[11] E. Chiellini, P. Cinelli, A. Corti, E.R. Kenawy, Composite films based on waste gelatin: thermal-mechanical properties and biodegradation testing, Polym. Degrad. Stab. 73 (2001) 549–555.
[12] R.J. Avena-Bustillos, B. Chiou, C.W. Olsen, P.J. Bechtel, D.A. Olson, T.H. Mchugh, Gelation, oxygen permeability, and mechanical properties of mammalian and fish gelatin films, J. Food Sci. 76 (2011) E519–E524.
[13] N. Benbettaïeb, M. Kurek, S. Bornaz, F. Debeaufort, Barrier, structural and mechanical properties of bovine gelatin-chitosan blend films related to biopolymer interactions, J. Sci. Food Agric. 94 (2014) 2409–2419.
[14] J. Biscarat, C. Charmette, J. Sanchez, C. Pochat-Bohatier, Gas permeability properties of gelatin/polyetheramine blend membranes made without organic solvent, Sep. Purif. Technol. 142 (2015) 33–39.
[15] R.A. De Carvalho, C.R.F. Grosso, Characterization of gelatin based films modified with transglutaminase, glyoxal and formaldehyde, Food Hydrocoll. 18 (2004) 717–726.
[16] J. Wu, S.-C. Chiu, E.M. Pearce, T.K. Kwei, Effects of phenolic compounds on gelation behavior of gelatin gels, J. Polym. Sci. A Polym. Chem. 39 (2001) 224–231.
[17] N. Cao, Y. Fu, J. He, Mechanical properties of gelatin films cross-linked, respectively, by ferulic acid and tannin acid, Food Hydrocoll. 21 (2007) 575–584.
[18] C. Ringwald, V. Ball, Step-by-step deposition of type B gelatin and tannic acid displays a peculiar ionic strength dependence at Ph 5, Rsc Adv. 6 (2016) 4730–4738.
[19] X. Zhang, M.D. Do, P. Casey, A. Sulistio, G.G. Qiao, L. Lundin, P. Lillford, S. Kosaraju, Chemical cross-linking gelatin with natural phenolic compounds as studied by high-resolution NMR spectroscopy, Biomacromolecules 11 (2010) 1125–1132.
[20] J. Zhao, F. Pan, P. Li, C. Zhao, Z. Jiang, P. Zhang, X. Cao, Fabrication of ultrathin membrane via layer-by-layer self-assembly driven by hydrophobic interaction towards high separation performance, ACS Appl. Mater. Interfaces. 5 (2013) 13275–13283.
[21] C. Peña, K. De La Caba, A. Eceiza, R. Ruseckaite, I. Mondragon, Enhancing water repellence and mechanical properties of gelatin films by tannin addition, Bioresour. Technol. 101 (2010) 6836–6842.
[22] B.-S. Chiou, R.J. Avena-Bustillos, P.J. Bechtel, H. Jafri, R. Narayan, S.H. Imam, G. M. Glenn, W.J. Orts, Cold water fish gelatin films: effects of cross-linking on thermal, mechanical, barrier, and biodegradation properties, Eur. Polym. J. 44 (2008) 3748–3753.
[23] I.C. Hahn Berg, D. Muller, T. Arnebrant, M. Malmsten, Ellipsometry and Tirf studies of enzymatic degradation of interfacial proteinaceous layers, Langmuir 17 (2001) 1641–1652.
[24] P. Dalev, E. Vassileva, J.E. Mark, S. Fakirov, Enzymatic degradation of formaldehyde-crosslinked gelatin, Biotechnol. Technol. 12 (1998) 889–892.
[25] M.C. Lu, S.W. Hsiang, T.Y. Lai, C.H. Yao, L.Y. Lin, Y.S. Chen, Influence of cross-linking degree of a biodegradable genipin-cross-linked gelatin guide on peripheral nerve regeneration, J. Biomater. Sci. Polym. Ed. 18 (2007) 843–863.
[26] J. Xiaohui, S. Xiangning, L. Jun, B. Yubai, Y. Wensheng, P. Xiaogang, Size control of gold nanocrystals in citrate reduction: the third role of citrate, J. Am. Chem. Soc. 129 (2007) 13939–13948.
[27] W. Haiss, N.T.K. Thanh, J. Aveyard, D.G. Fernig, Determination of size and concentration of gold nanoparticles from Uv−Vis spectra, Anal. Chem. 79 (2007) 4215–4221.
[28] A.J. Bard, L.R. Faulkner, Electrochemical Methods. Fundamental and Applications, second ed., Wiley, Ny, 2001.
[29] M. Rodahl, F. Höök, C. Fredriksson, C.A. Keller, A. Krozer, P. Brzezinski, M. Voinova, B. Kasemo, Simultaneous frequency and dissipation factor Qcm measurements of biomolecular adsorption and cell adhesion, Faraday Discuss. 107 (1997) 229–246.
[30] M. Rodahl, F. Höök, A. Krozer, P. Brzezinski, B. Kasemo, Quartz crystal microbalance setup for frequency and Q-factor measurements in gaseous and liquid environments, Rev. Sci. Instrum. 66 (1995) 3924–3930.
[31] G. Sauerbrey, Verwendung Von Schwingquarzen Zur Wägung Dünner Schichten Und Zur Mikrowägung, Z. Physik 155 (1959) 206–222.
[32] L. Macakova, E. Blomberg, P.M. Claesson, Effect of adsorbed layer surface roughness on the Qcm-D response: focus on trapped water, Langmuir 23 (2007) 12436–12444.
[33] M.V. Voinova, M. Rodahl, M. Jonson, B. Kasemo, Viscoelastic acoustic response of layered polymer films at fluid-solid interfaces: continuum mechanics approach, Phys. Scr. 59 (1999) 391–396.
[34] A. Delvar, L. Lindh, T. Arnebrant, J. Sotres, Interaction of polyelectrolytes with salivary pellicles on hydroxyapatite surfaces under erosive acidic conditions, ACS Appl. Mater. Interfaces. 7 (2015) 21610–21618.
[35] T.P. Vikinge, K.M. Hansson, P. Sandström, B. Liedberg, T.L. Lindahl, I. Lundström, P. Tengvall, F. Höök, Comparison of surface plasmon resonance and quartz crystal microbalance in the study of whole blood and plasma coagulation, Biosens. Bioelectron. 15 (2000) 605–613.
[36] I. Erel-Unal, S.A. Sukhishvili, Hydrogen-bonded multilayers of a neutral polymer and a polyphenol, Macromolecules 41 (2008) 3962–3970.
[37] F. Höök, B. Kasemo, T. Nylander, C. Fant, K. Sott, H. Elwing, Variations in coupled water, viscoelastic properties, and film thickness of a Mefp-1 protein film during adsorption and cross-linking: a quartz crystal microbalance with dissipation monitoring, ellipsometry, and surface plasmon resonance study, Anal. Chem. 73 (2001) 5796–5804.
[38] J. Sotres, A. Barrantes, L. Lindh, T. Arnebrant, Strategies for a direct characterization of phosphoproteins on hydroxyapatite surfaces, Caries Res. 48 (2014) 98–110.
[39] M. Keeney, X.Y. Jiang, M. Yamane, M. Lee, S. Goodman, F. Yang, Nanocoating for biomolecule delivery using layer-by-layer self-assembly, J. Mater. Chem. B Mater. Biol. Med. 3 (2016) 8757–8770.
[40] V.G.L. Souza, A.L. Fernando, Nanoparticles in food packaging: biodegradability and potential migration to food—a review, Food Packag. Shelf Life 8 (2016) 63–70.